FEBS 24645 FEBS Letters 491 (2001) 305–311

Genetic and functional linkage of Kir5.1 and Kir2.1 channel subunits

Christian Derst[a], Christine Karschin[b], Erhard Wischmeyer[b], Jochen R. Hirsch[d], Regina Preisig-Müller[a], Sindhu Rajan[a], Hartmut Engel[c], Karl-Heinz Grzeschik[c], Jürgen Daut[a], Andreas Karschin[b,*]

[a] *Institute for Normal and Pathological Physiology, University of Marburg, 35033 Marburg, Germany*
[b] *Department of Molecular Neurobiology of Signal Transduction, Max-Planck-Institute for Biophysical Chemistry, 37070 Göttingen, Germany*
[c] *Institute for Human Genetics, University of Marburg, 35033 Marburg, Germany*
[d] *Medical Policlinic, Experimental Nephrology, University of Münster, 48149 Münster, Germany*

Received 17 October 2000; revised 31 January 2001; accepted 31 January 2001

First published online 14 February 2001

Edited by Takashi Gojobori

Abstract We have identified several cDNAs for the human Kir5.1 subunit of inwardly rectifying K^+ channels. Alternative splicing of exon 3 and the usage of two alternative polyadenylation sites contribute to cDNA diversity. The hKir5.1 gene *KCNJ16* is assigned to chromosomal region 17q23.1–24.2, and is separated by only 34 kb from the hKir2.1 gene (*KCNJ2*). In the brain, Kir5.1 mRNA is restricted to the evolutionary older parts of the hindbrain, midbrain and diencephalon and overlaps with Kir2.1 in the superior/inferior colliculus and the pontine region. In the kidney Kir5.1 and Kir2.1 are colocalized in the proximal tubule. When expressed in *Xenopus* oocytes, Kir5.1 is efficiently targeted to the cell surface and forms electrically silent channels together with Kir2.1, thus negatively controlling Kir2.1 channel activity in native cells.

Key words: Inwardly rectifying K^+ channel; Kir5.1; *KCNJ16*; Kir2.1; In situ hybridization; Chromosomal localization

1. Introduction

The family of inwardly rectifying potassium (Kir) channels comprises several well-defined subfamilies, e.g. weakly rectifying Kir1/Kir4 channels, strongly voltage-dependent Kir2 channels, G protein-gated Kir3 channels and ATP/MgADP-controlled Kir6 channels [1]. Primarily based on significant structural differences, two further subunits, Kir5.1 and Kir7.1, were grouped separately. Kir7.1 subunits present in the epithelia of several central and peripheral tissues have now been recognized to form Kir channels with a non-conserved pore region that results in unique unitary and macroscopic permeation and rectification properties [2–6]. Yet, much less is known about the function of Kir5.1 subunits, which have been found by reverse transcription (RT)-PCR in the adrenal gland, spleen, liver, kidney, testis, and brain [7,8]. First attempts to express Kir5.1 in heterologous expression systems failed to generate K^+ currents [7]. Coexpression studies, however, demonstrated that Kir5.1 subunits assembled into functional heteromeric complexes together with Kir4.1/1.2 [9] and Kir4.2/1.3 subunits [10].

Here we report novel cDNA sequences for the rat (rKir5.1) and human Kir5.1 (hKir5.1) subunits as well as the complete genomic structure of the hKir5.1 gene *KCNJ16*. Based on the finding that *KCNJ16* is colocalized with the Kir2.1 gene (*KCNJ2*) on chromosomal region 17q23.1–24.2 we investigate a putative functional linkage between Kir5.1 and Kir2.1 subunits in mammalian tissues.

2. Materials and methods

2.1. Database and sequence analysis

The complete human gene encoding the Kir5.1 subunit *KCNJ16* was identified from a large genomic GenBank database entry of chromosome 17 (GenBank accession number AC005208) using the BLAST algorithm [11] and the originally published cDNA sequence of rKir5.1 (X83581). To obtain cDNA information, EST databases were analyzed and several partial but overlapping IMAGE-EST clones encoding hKir5.1 were obtained from the Resource Center of the German Human Genome Project (RZPD) at the Max-Planck-Institute for Molecular Genetics, Berlin, Germany, and completely sequenced.

2.2. RT-PCR analysis

To assay alternative splicing events in the 5′ untranslated region (UTR) of hKir5.1, human kidney RNA was reverse-transcribed using Superscript II reverse transcriptase (Gibco BRL) and used as template for RT-PCR. For RT-PCR analysis of human renal tissue fractions, dissected tubules of 200 mm in total length and 400 glomeruli were lysed in 4 M guanidinium buffer and total RNA was isolated using the RNeasy kit (Qiagen, Hilden, Germany). After DNaseI (Promega, Heidelberg, Germany) digestion RNA was reverse-transcribed using MMLV reverse transcriptase (Promega). Amplifications were performed using intron-spanning primers localized on exons 2 and 4 of Kir5.1 (132 bp), and on exons 1 and 2 for Kir2.1 (199 bp), respectively (Kir5.1: 5′-AGGATTCTAACTGGCAGACTGG-3′; 5′-GATTTCCCAGCTCAAGTCAAAG-3′, Kir2.1: 5′-TCTTGGGAATTCTGGTTTGC-3′; 5′-TGGGAGCCTTGTGGTTCTAC-3′), with 94°C denaturation, 52°C annealing and 72°C elongation (30 s each) for 35 cycles using AmpliTaq Gold Polymerase (Perkin Elmer, Weiterstadt, Germany). All PCR products were directly sequenced to confirm correct amplification. As described before in detail [12] GAPDH-specific PCRs were performed as positive controls with reverse transcriptase reactions from all nephron segments. As negative controls reverse transcriptase was omitted. To exclude contaminations, appropriate water controls excluding cDNAs were additionally performed.

2.3. Chromosomal assignment of KCNJ16

The exact position of *KCNJ16* on chromosome 17 was identified using a 339 bp PCR fragment (containing exon 2) which was amplified from a Stanford TNG4 radiation hybrid panel [13] using the

*Corresponding author. Fax: (49)-551-2011688.
E-mail: akarsch@gwdg.de

PII: S0014-5793(01)02202-5

following amplification primers: FOR: 5′-AGCAGCTCCACATAGAAAAAGC-3′, BACK: 5′-TAACACTTTCAAAAAAGCCACG-3′. The resulting data vector was analyzed using RH mapping at the Stanford Human Genome Center (http://www-shgc.stanford.edu/Mapping/rh/index.html), the GeneMap 99 at the National Center for Biotechnology Information (http://www.ncbi.nlm.nih.gov/genemap) and the Genome Database (http://www.gdb.org).

2.4. In situ hybridization of Kir5.1 in rat brain

In situ hybridizations with Kir5.1 probes and all appropriate controls were performed on 16 μm cryostat brain sections of adult Wistar rats as described in detail elsewhere [14]. Here, synthetic antisense oligonucleotides were chosen from both the UTR and open reading frame (ORF) of rKir5.1 [7] with least tendency of forming hairpins and self-dimers (coding strand positions indicated): 5′UTR: 5′-$^{-50}$CGTGCTTGCAGCTCAGGGCCTTCAGGTAAGGGTCAGAGAGGAGGG^{-1}-3′ and ORF: 5′-^{1254}CTGGGATTCCATGGAGATCCTGTTTAAAGTCAGGAGGGC^{1216}-3′. Parallel sections were hybridized to oligonucleotide probes specific for Kir2.1 as previously published [14]. In brief, oligonucleotides were 3′ end-labeled with [^{35}S]dATP or [^{33}P]dATP (New England Nuclear, Boston, MA, USA; 1200 and 1000 Ci/mmol) by terminal deoxynucleotidyl transferase (Roche Diagnostics, Mannheim, Germany) and used for hybridization at concentrations of 2–10 pg/μl ($4{\cdot}10^5$ cpm/100 μl hybridization buffer per slide). Slides were air-dried and hybridized for 20–24 h at 43°C in 100 μl buffer containing 50% formamide, 10% dextran sulfate, 50 mM dithiothreitol, 0.3 M NaCl, 30 mM Tris–HCl, 4 mM EDTA, 1×Denhardt's solution, 0.5 mg/ml denatured salmon sperm DNA, and 0.5 mg/ml polyadenylic acid and labeled oligonucleotide probe. Sections were washed 2×30 min in 1×SSC plus 50 mM β-mercaptoethanol, 1 h in 1×SSC at 60°C, and 10 min in 0.1×SSC at room temperature. Specimens were then dehydrated, air-dried and exposed to Kodak BIOMAX X-ray film for 16–28 days. For cellular resolution, selected slides were dipped in photographic emulsion Kodak NTB2, incubated for 8–16 weeks and then developed in Kodak D-19 for 2.5 min. For identification of brain structures with bright- and dark-field optics, sections were Nissl-counterstained with cresyl violet [15].

2.5. Construction of Kir5.1 expression vectors

For expression, the coding regions of rKir5.1 and hKir5.1 were PCR-amplified using primers containing start and stop codons, respectively (hKir5.1-FOR: 5′-AGAATGAGCTATTACGGCAGCAGC-3′; hKir5.1-BACK: 5′-CAGTGGTAGCCCTCATAATTGC-3′; rKir5.1-FOR: 5′-ATGAGCTATTACGGAAGTAGC-3′; rKir5.1-BACK: 5′-CTACATCTGGGATTCCATGGA-3′). The PCR profile was 94°C, 52°C (30 s each), 72°C (2 min) for 30 cycles using AmpliTaq Gold Polymerase (Perkin Elmer). PCR products were sequenced and blunt-end ligated into the *Xenopus* expression vector pSGEM (a gift of Dr. M. Hollmann, Göttingen, Germany). In addition, hKir2.1 and hKir5.1 cDNAs were fused to the gene encoding the enhanced green fluorescence protein (EGFP) in pEGFP-C1 (Clontech) and then subcloned into pSGEM.

2.6. Electrophysiological analysis

For expression in *Xenopus laevis* oocytes capped run-off poly(A)$^+$ cRNA transcripts were synthesized from wild-type and mutant Kir5.1, Kir2.1, and Kir2.1–Kir5.1 concatemers, and injected individually (~3 ng each) or in combination (with Kir2.1 cRNA held constant) in defolliculated oocytes. Oocytes were incubated at 19°C in ND96 solution (96 mM NaCl, 2 mM KCl, 1 mM $MgCl_2$, 1 mM $CaCl_2$, 5 mM HEPES, pH 7.4–7.5), supplemented with 100 μg/ml gentamicin and 2.5 mM sodium pyruvate, and assayed 48 h after injection. Two-electrode voltage-clamp measurements were performed with a Turbo Tec-10 C amplifier (npi, Tamm, Germany) and sampled through an EPC9 (Heka Electronics, Lambrecht, Germany) interface using Pulse/Pulsefit software (Heka). Oocytes were placed in a small-volume perfusion chamber and bathed with ND96 or 'high K^+' solution (96 mM KCl, 2 mM NaCl, 1 mM $MgCl_2$, 1 mM $CaCl_2$, 5 mM HEPES, pH 7.4–7.5).

For cell-attached single-channel recordings patch pipettes were pulled from borosilicate glass capillaries (Hilgenberg, Malsfeld, Germany), Sylgard©-coated (Dow Corning, USA), and heat-polished to give input resistances of 1–2 MΩ. The pipette recording solution contained 120 mM KCl, 10 mM HEPES, and 1.8 mM $CaCl_2$ (pH 7.3), and the bath solution was changed to 120 mM KCl, 10 mM HEPES, 10 mM EGTA, 2.4 mM $MgCl_2$, 1.13 mM Na_2ATP. Using Pulse/Pulsefit currents were recorded in voltage-clamp with an EPC9 patch clamp amplifier (Heka) and low pass-filtered at 1–2 kHz.

3. Results

3.1. Cloning of hKir5.1

A GenBank database homology search with rKir5.1 identified a large genomic database entry of chromosome 17 harboring *KCNJ16*. Based on this sequence information two overlapping cDNA clones encoding hKir5.1 were retrieved from an EST database and assembled into a 2089 bp long cDNA clone including a polyadenylation signal (AATAAA) preceding the poly(A)$^+$ stretch (Fig. 1). The resulting ORF encodes a protein of 418 amino acids which is 34 amino acids longer than the Kir5.1 sequence originally identified from rat brain [7]. Since we amplified ORFs of 1254 bp from both rat and human templates we interpret the cDNA sequence described by Bond et al. [7] to be truncated, possibly due to a frameshift error at residue 351. At the amino acid level, hKir5.1 is 91% identical to both rKir5.1 and the recently published mouse Kir5.1 [16]. Based on the novel sequences, Kir5.1 now appears most closely related to members of the Kir2 family, with 43% (56% nucleotide similarity) identity to Kir2.1 [17], 42% (53%) identity to Kir2.2 [18], 41% (55%) identity to Kir2.3 [19] and 40% (51%) identity to Kir2.4 [20].

3.2. Genomic structure of KCNJ16

Analysis of the genomic structure of *KCNJ16* and comparison to an EST clone from a parathyroid tumor database revealed that the terminal 5′UTR of the cDNA is encoded by four small exons of 106 bp (exon 1), 109 bp (exon 2), 81 bp (exon 3) and 97 bp (exon 4). The fifth exon is much larger (1681 bp) and harbors the remaining 5′UTR, the entire coding region and the complete 3′UTR (Fig. 2). Direct sequencing of the exon–intron boundaries showed that donor and acceptor splice sites are conserved in all cases (GT/AG; Fig. 2B).

The sequences of intron 1 (25 267 bp), intron 2 (7534 bp), intron 3 (22 497 bp), and intron 4 (1019 bp) show multiple repetitive elements. Within intron 2, exon 3 appears to be duplicated approximately 1.6 kb upstream (Fig. 2). The putative exon 3b is 90% identical to exon 3, and has conserved 5′ and 3′ splice sites, however, it has not been found in any EST clone or PCR amplification product of various tissues. Moreover, when the stretch around exon 3 was analyzed by RT-PCR from human kidney RNA, neither exon 3 nor 3b was found in the cDNA. Thus, in kidney, a tissue-specific splicing mechanism results in a shorter hKir5.1 variant of 1856 bp (Fig. 2).

An alternative polyadenylation event was detected in several partial hKir5.1 clones from parathyroid tumor, kidney, brain and thyroid cDNA libraries (Fig. 2). In this case ~2 kb are added to the 3′ end beyond the first polyadenylation signal resulting in a hKir5.1 cDNA of 4021 bp.

3.3. hKir2.1 cDNA and gene structure

Remarkably, another overlapping DNA fragment from chromosome 17 was found to contain *KCNJ2*, the gene that encodes the hKir2.1 subunit (Fig. 2). Sequence comparison of *KCNJ2* with the hKir2.1 cDNA [16] revealed that the 5′UTR is split by a single intron (4311 bp) with several repetitive

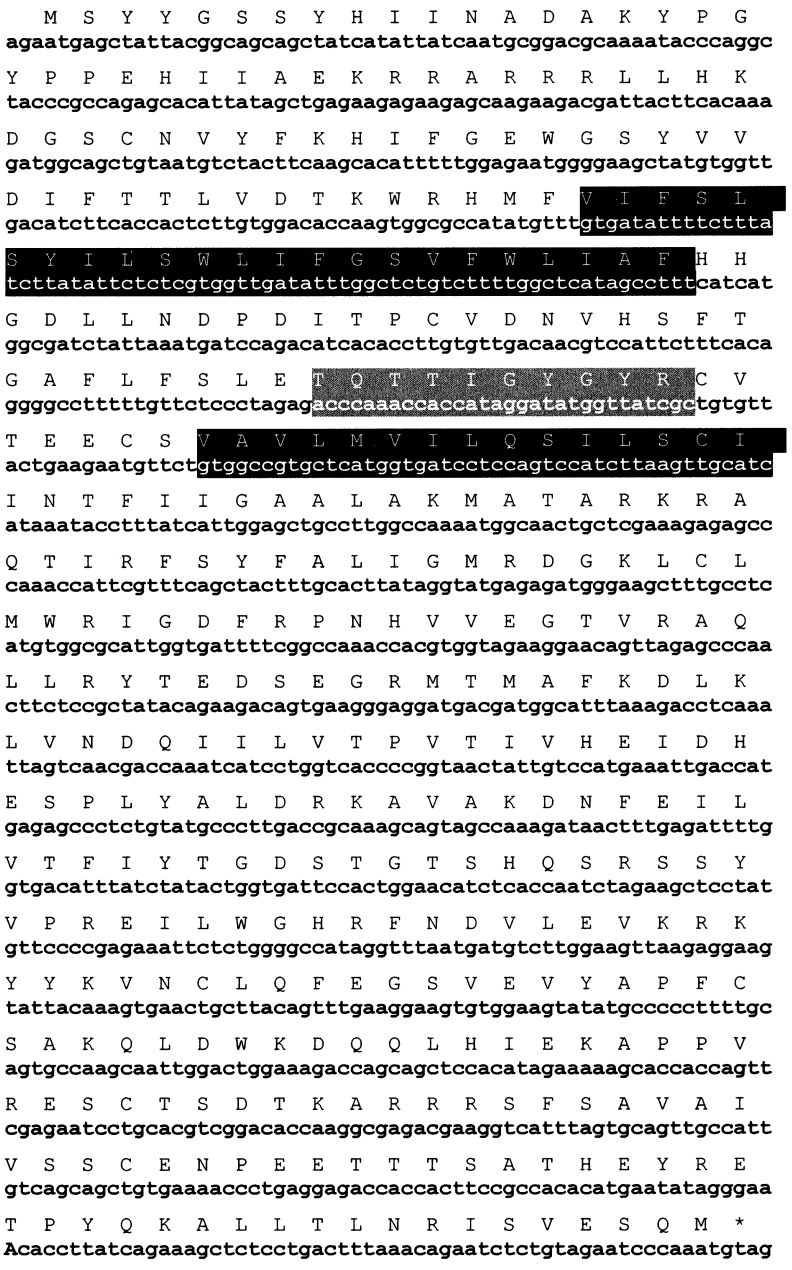

Fig. 1. cDNA sequence of the hKir5.1/*KCNJ16* gene. The full-length sequence is assembled from two EST clones (AA846603, AI271845) and has been submitted to GenBank under the accession number AF153815. The ORF encodes a protein with 418 amino acids with two predicted transmembrane regions (M1, M2; boxed in black) and a pore-forming structure (P1; boxed in gray). Amino acid sequence is shown in the single-letter code. Note that the hKir5.1 sequence is extended by 34 amino acids compared to rKir5.1 sequence published originally.

elements. In *KCNJ2*, exon 1 (166 bp) is preceded by a region homologous to the rat *KCNJ2* promotor region [21], and exon 2 (5220 bp) contains the remaining 5′UTR, the coding region (which is 98% identical to the rat and mouse sequence), and the 3′UTR with the polyadenylation signal, predicting a total cDNA sequence of ~5.4 kb. Between the end of *KCNJ16* and the transcriptional start site of *KCNJ2* (deduced by homology to the mouse Kir2.1 [16]) there are only 34 kb, indicating an ancient gene duplication event in evolution.

3.4. Assignment to chromosomal region 17q23.1–24.2

To identify the exact chromosomal position of hKir5.1, the Stanford radiation hybrid panel [13] was analyzed. *KCNJ16* was mapped to chromosome 17, 53 cR_{50000} from the flanking markers SHGC-78842 and 74 cR_{50000} from SHGC-79125 (Table 1). Electronic PCR places these markers proximal and distal of the Kir2.1 and Kir5.1 loci within BAC clones AC005242 and AC004562, respectively. These clones are part of contig NT-001524 which can be placed on the GeneMap 99 physically to the interval D17S795–D17S840, 90.2–94.8 cM from the pter of chromosome 17, by microsatellite marker D17S1786 (AFMa112yb5) and the gene marker map kinase 6 (MAP2K6). According to the Genome Database this interval corresponds to the cytogenetic map in the region 17q23.1–17q24.2.

3.5. Distribution of Kir5.1 in the rat brain

To date, the cellular distribution pattern of Kir5.1 in mam-

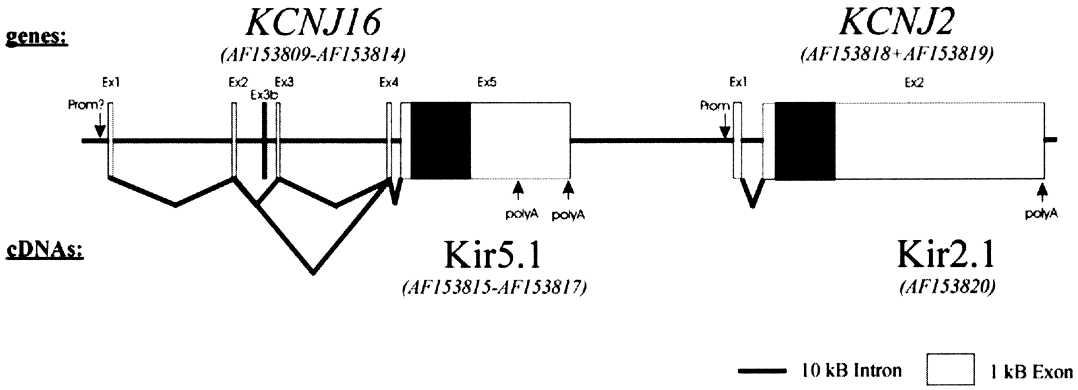

Fig. 2. Genomic organization of the human *KCNJ16*/*KCNJ2* gene cluster located on chromosome 17q23.1–24.3. (A) *KCNJ16* is ~60 kb in length and contains five (+one putative) exons (GenBank accession numbers AF153809–AF153814), *KCNJ2* is ~10 kb in length and consists of two exons (GenBank accession numbers AF1538218–AF1538220). Coding regions are shown as black boxes, non-coding regions as white boxes, the putative exon 3b of *KCNJ16* is denoted. For clarity intronic sequences (taken from genomic GenBank entries AC005208 and AC005242) have been reduced 10-fold compared to exon size. Note that exon 5 of *KCNJ16* is only 34 kb upstream of the *KCNJ2* transcriptional start site. Positions of polyadenylation sites and putative promotor regions are indicated by arrows.

malian brain has not been analyzed. Because of the close proximity of Kir5.1 and Kir2.1 we were interested in comparing their localization in the rat brain by in situ hybridization. Analysis of the hybridization signals in sagittal and coronal sections showed that expression of Kir5.1 was restricted to the more ancient parts of the brain: hindbrain, midbrain and diencephalon (Fig. 3). In this respect Kir5.1 differs from all other Kir channels localized in the brain so far. The strong and homogenous Kir5.1 expression indicates expression both in neurons and glia. Whereas at high resolution no signal was found in oligodendrocytes, small-size astrocytes were clearly labeled, for example in the facial nucleus and other nuclei containing large motoneurons but no small interneurons, or at the border of the molecular and Purkinje cell layer of the cerebellum. Further non-neuronal structures such as the ependymal layers lining the ventricles were also found positive.

In contrast, the complete cerebral hemisphere including the cortex, hippocampal formation, basal ganglia and amygdala was largely unlabeled. Notable exceptions were moderate signals in a population of layer V neurons in the forelimb and hindlimb of the cortex and the retrosplenial cortex, as well as in the hippocampal CA1 and dentate gyrus granule cell layer.

In situ hybridization analysis with Kir2.1-specific probes performed here and in an earlier study [14] demonstrated that Kir2.1 coexpresses with Kir5.1 at some distinct sites in the anterior pretectal nucleus, in the superior and inferior colliculus, and in the pontine nucleus (e.g. Fig. 3D).

3.6. Distribution of Kir5.1 and Kir2.1 in the human kidney

When assayed by RT-PCR, hKir5.1 expression was found in the proximal tubule, the thick ascending limb and the cortical collecting duct of human kidney (Fig. 4), but was absent from isolated glomeruli. On the other hand, Kir2.1 signals were only detected in isolated glomeruli and in the proximal tubule system (Fig. 4). Thus, in human kidney both subunits are coexpressed only in the proximal part of the tubule system, as shown in the diagram (Fig. 4B).

3.7. Functional expression of hKir5.1

Previous studies in *Xenopus* oocytes have documented that rKir5.1 fails to form functional homomeric channels, but requires specific coassembly with Kir4.1/Kir4.2 subunits [7,9]. One possible explanation for the lack of functional expression of Kir5.1 is that a retention signal prevented the targeting to the surface membrane (analogous to the retention signal (RKR) recently detected in the C-terminus of Kir6 subunits [22–24]). Indeed, we identified two putative retention signals at positions 317 (KRK) and 370 (RRR) in the hKir5.1 C-terminus, respectively. However, when these sites were replaced by glycine residues, individually or in combination, the modified hKir5.1 subunits still failed to express functional channels in oocytes ($n = 10$ each).

In another set of experiments we tagged hKir5.1 with EGFP at the NH_2-terminus to investigate its subcellular localization. cRNAs of EGFP-hKir5.1 and EGFP-Kir2.1 were injected into oocytes and membrane fluorescence was studied by confocal microscopy. After 48 h we found strong membrane fluorescence (quantified by line-scan luminometry) which was indistinguishable for injection of Kir2.1, Kir5.1 or a 1:1 combination of both (Fig. 5B, inset). Despite their obvious local-

Table 1
Stanford TNG4 panel radiation hybrid mapping data

Gene/locus	Primer pair (product size)	Data vector[a]	Flanking marker	Physical distance	Lod score	Cytogenetic map location	GeneMap 99 interval
Kir5.1	Kir5.1ex2 for, Kir5.1ex2 rev	00000000100000000101000011010000001100110011000001000011001110000000011100000000000010000	SHGC-78842	53 cR_{50000}	6.34	17q23.1–17q24.2	D17S795–D17S840
			SHGC-79125	74 cR_{50000}	4.01		

[a]0, negative; 1, positive.

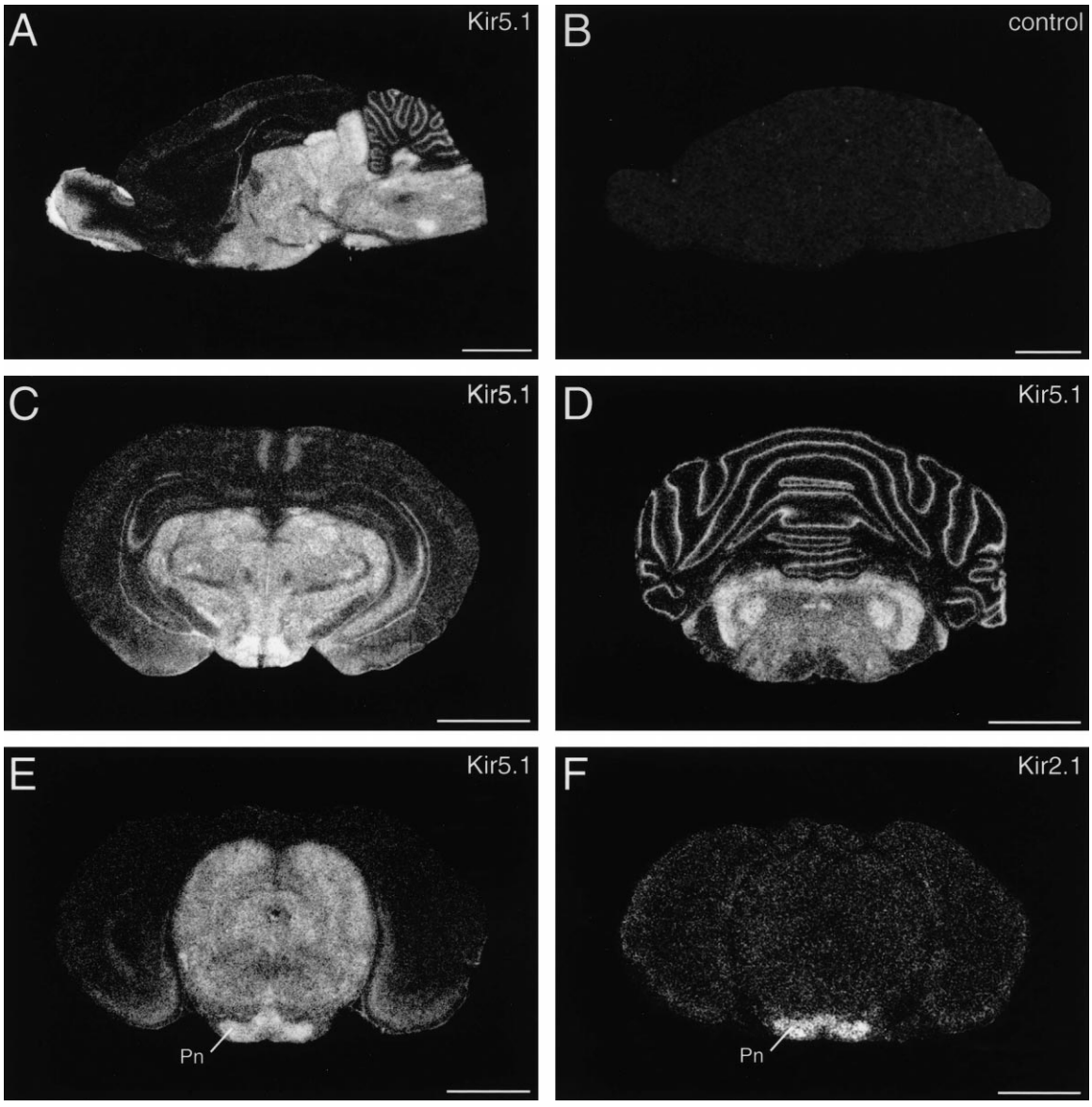

Fig. 3. In situ hybridization of Kir5.1 and Kir2.1 mRNAs in the rat brain. Sections were hybridized with ^{33}P-labeled specific oligonucleotides as described in Section 2. X-ray film autoradiographs of a sagittal (A,B) and transversal sections (C–F) show Kir5.1 mRNA primarily restricted to the midbrain, hindbrain and diencephalon (A,C,D,E), and strong coexpression of Kir2.1 mRNAs (F) in the pontine region (Pn). (B) No signal is present in a control section digested with RNase A prior to hybridization with Kir5.1-specific probes. Exposure time was 26 days. Scale bars represent 4 mm (A,B), 3 mm (C–F).

ization in the membrane hKir5.1 subunits fail to form functional channels. Nevertheless, we obtained evidence for interaction of Kir5.1 subunits with Kir2.1, in contrast to previous findings [9]. When Kir2.1 and Kir5.1 cRNAs were injected at equimolar amounts ($n > 10$), all macroscopic current properties were virtually indistinguishable from Kir2.1 currents, but the current amplitude at -100 mV was reduced to 63% (from -22.7 ± 7.4 μA to -14.3 ± 2.2 μA). Injection of larger amounts of Kir5.1 cRNA (with Kir2.1 cRNA kept constant) further decreased the macroscopic current amplitude. At a Kir5.1/Kir2.1 cRNA ratio of 2:1 Kir2.1 activity was suppressed to 43% (-9.5 ± 2.4 μA), at a Kir5.1/Kir2.1 ratio of 5:1 the current amplitude was reduced to 5% (-0.09 ± 0.02 μA; $n = 10$ each; Fig. 5A,C). In contrast, no effect was observed on the macroscopic amplitudes of Kir1.1 (ROMK) currents, when Kir5.1 cRNA was coinjected. Moreover, no channel activity was detected in oocytes after injection of engineered Kir2.1–Kir5.1 dimers. Additional evidence for a molecular interaction between the two subunit species was obtained from experiments using mutant Kir5.1 subunits in which the pore signature GYG was changed to VYG (Kir5.1G133V) to further disturb channel function. When Kir5.1G133V cRNA was coinjected with Kir2.1 at a 1:1 ratio the macroscopic current amplitudes were only 39% of the Kir2.1 control (white bar in Fig. 5), which is a statistically significant reduction compared to wild-type Kir5.1 subunits (Student's t test; $P < 0.01$). Single-channel cell-attached recordings revealed that oocytes coinjected with Kir5.1 and Kir2.1 at a 1:1 ratio exhibited only one additional single-channel population with a unitary conductance typical of homomeric Kir2.1 channels ($\gamma = 27$ pS; $n = 15$). In summary, these data support the notion that Kir5.1 subunits coassemble

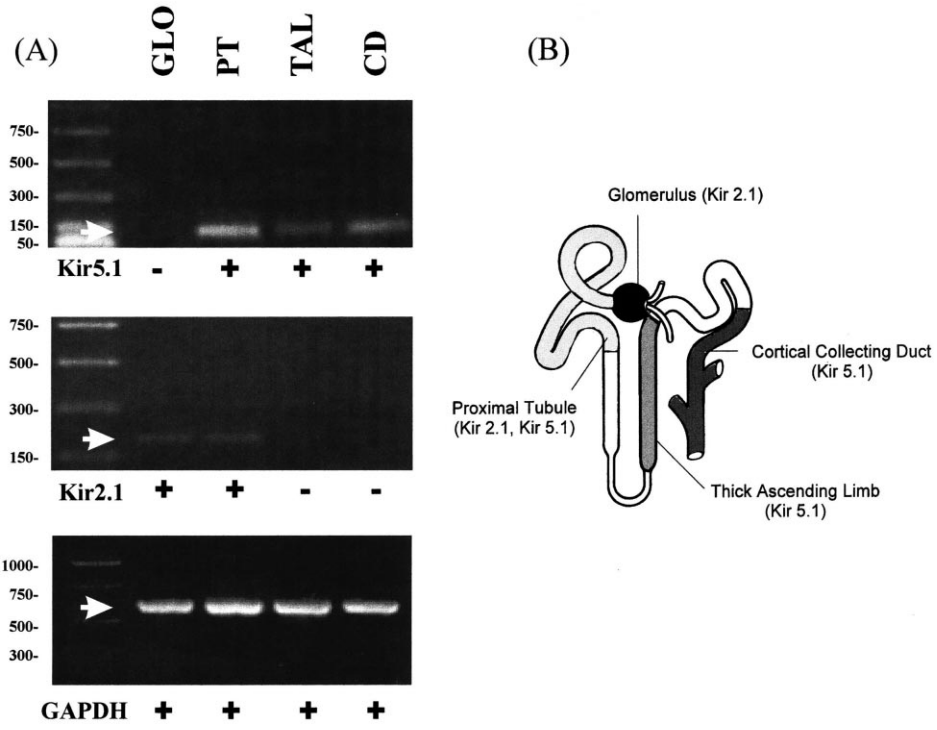

Fig. 4. Expression of hKir5.1 and hKir2.1 subunits in human kidney. (A) RT-PCR analysis of human glomeruli (GLO), proximal tubules (PT), thick ascending limbs (TAL), and cortical collecting ducts (CD). Also shown is a molecular weight marker (left lane). White arrows denote the size of correct PCR fragments. As shown in the bottom panel all RT samples were positive for GAPDH, indicating integrity of isolated RNAs and successful reverse transcription. Negative controls were performed with all RNA samples to exclude contaminations. (B) Schematic diagram of hKir5.1 and hKir2.1 expressed in the different segments of the nephron.

with Kir2.1 to form electrically silent channels and thus function as negative regulators of the Kir2.1 conductance.

4. Discussion

Our finding that in man the genes for Kir5.1 (*KCNJ16*) and Kir2.1 (*KCNJ2*) are colocalized on chromosome 17q in close proximity is paralleled in the mouse where Kir5.1 [16] and Kir2.1 [25] have been mapped to the distal region of chromosome 11 (also found on the single unmapped mouse genomic database entry AC025586), which shares homology with human chromosome 17q. Thus, the chromosomal association of Kir5.1 and Kir2.1 is similar to other pairs of Kir subunits that in humans are colocalized on the same chromosomal arm and may be an indication for an early gene duplication event [26]. The high similarity in primary sequence and functional properties of subunits within the subfamilies suggest that an ancient intrachromosomal gene duplication event separating two members of the Kir family has taken place prior to copying these pairs to different chromosomal locations, thereby forming Kir subfamilies. The lower homology between Kir2.1 and Kir5.1 (43% and 56% identity at the amino acid and nucleo-

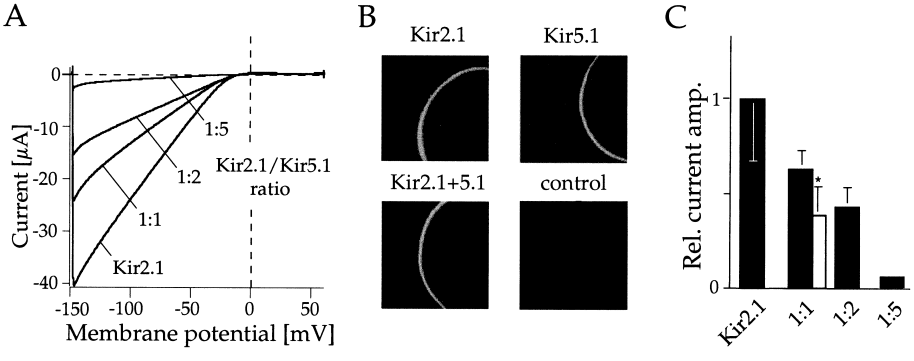

Fig. 5. Coexpression of hKir5.1 and Kir2.1 subunits in *Xenopus* oocytes. (A) Ramp recordings (2 s) from *Xenopus* oocytes injected with Kir2.1 cRNA individually, or in combination with hKir5.1 cRNA at the ratios indicated (with constant amounts of Kir2.1 cRNA). (B) Confocal images of the membrane fluorescence of oocytes injected with EGFP-Kir2.1, EGFP-Kir5.1, EGFP-Kir2.1+Kir5.1, and water (control), respectively. Laser-scan images were taken from the animal pole on an Axiovert 135 microscope equipped with an argon–crypton laser with a 16× oil objective lens. (C) Bar graph showing the mean current amplitudes ($n = 10$) from oocytes injected with Kir2.1 alone and together with Kir5.1 at the ratios indicated. The open bar is the result of Kir2.1 coinjected with mutant Kir5.1G133V subunits (asterisk denotes statistical significance at the 0.01% level).

tide level, respectively), compared to the homologies among members of the same subfamily, may be the result of a long independent evolutionary process following the first intrachromosomal duplication.

In relation to the present study it is intriguing that the hKir2.2 gene (*KCNJ12*) which is also located on chromosome 17 (17p11.1) has been copied to encode a protein hKir2.2v (*KCNJN1*) which exhibits 95% amino acid similarity [27], but represents a silent gene product when expressed by itself and acts as a negative regulator of the hKir2.2 channel activity [28]. By analogy, we may speculate from the sequence similarity that Kir5.1 is a doublet of Kir2.1 that has adopted a similar modulatory function early in evolution.

In agreement with a recent immunochemical analysis with Kir5.1-specific antibodies [8], our confocal localization studies in *Xenopus* oocytes with EGFP-tagged Kir5.1 indicate that Kir5.1 subunits are normally synthesized and transported to the surface membrane. When assembled with Kir4.1/4.2 subunits, Kir5.1 subunits form functional channels in a preferred 4-5-4-5 stoichiometry with altered gating kinetics, increased macroscopic amplitude and single-channel conductance [9,10]. Moreover, the activity of Kir4.1/5.1 channels is completely blocked by internal acidification $<$ pH 7 which may cause the channels to function as physiological pH sensors [29,30]. Thus, both in peripheral tissues (e.g. kidney, liver, spleen, adrenal gland and testis), and in the brain (where both mRNA species appear to be colocalized in glial and epithelial cells [31]), Kir5.1 forms a conducting channel pore when complexed together with Kir4.1 but suppresses the activity of Kir2.1 channels. The microscopically identified localization at the cell surface and our functional data suggest that Kir5.1 subunits indeed incorporate into silent heteromeric channel complexes together with Kir2.1, rather than suppressing the expression and transport of Kir2.1 subunits by other mechanisms. Thus, in native tissue where Kir5.1 is strongly coexpressed with Kir2.1, for example, in the pontine region of the brain or the proximal tubule of the kidney, it is quite likely that Kir5.1 subunits act as a negative regulator of the Kir2.1 conductance.

Acknowledgements: We thank Anette Hennighausen and Dirk Reuter for excellent technical assistance. This work was supported in part by the Deutsche Forschungsgemeinschaft Grants Da177/7-3 and Ka1175/1-3 and the P.E. Kempkes Stiftung.

References

[1] Isomoto, S., Kondo, C. and Kurachi, Y. (1997) Jpn. J. Physiol. 47, 11–39.
[2] Krapivinsky, G., Medina, I., Eng, L., Krapivinsky, L., Yang, Y. and Clapham, D.E. (1998) Neuron 20, 995–1005.
[3] Döring, F., Derst, C., Wischmeyer, E., Karschin, C., Schneggenburger, R., Daut, J. and Karschin, A. (1998) J. Neurosci. 18, 8625–8636.
[4] Partiseti, M., Collura, V., Agnel, M., Culouscou, J.-M. and Graham, D. (1998) FEBS Lett. 434, 171–176.
[5] Nakamura, N., Suzuki, Y., Sakuta, H., Ookata, K., Kawahara, K. and Hirose, S. (1999) Biochem. J. 342, 329–336.
[6] Wischmeyer, E., Döring, F. and Karschin, A. (2000) FEBS Lett. 466, 115–120.
[7] Bond, C.T., Pessia, M., Xia, X.M., Lagrutta, A., Kavanaugh, M.P. and Adelman, J.P. (1994) Recept. Channels 2, 183–191.
[8] Salvatore, L., D'Adamo, M.C., Poishchuck, R., Salmona, M. and Pessia, M. (1999) FEBS Lett. 449, 146–152.
[9] Pessia, M., Tucker, S.J., Lee, K., Bond, C.T. and Adelman, J.P. (1996) EMBO J. 15, 2980–2987.
[10] Pearson, W.L., Dourado, M., Schreiber, M., Salkoff, L. and Nichols, C.G. (1999) J. Physiol. 514, 639–653.
[11] Altschul, S.F., Madden, T.L., Shaffer, A.A., Zjang, J., Miller, W. and Lipman, D.J. (1997) Nucleic Acids Res. 25, 3389–3402.
[12] Schulte, E.A., Hohendahl, A., Stegemann, H., Hirsch, J.R., Saleh, H. and Schlatter, E. (1999) Cell. Physiol. Biochem. 9, 310–322.
[13] Beasley, E.M., Stewart, E.A., McKusick, K.B., Aggarwal, A., Brady-Hebert, S., Fang, N.Y., Lewis, S.C., Lopez, F., Norton, J., Pabla, H., Perkins, S.M., Piercy, M., Qin, F., Reif, T., Sun, W.-L., Vo, N., Myers, R.M. and Cox, D.R. (1997) ASHG abstract #1338.
[14] Karschin, C., Dissmann, E., Stühmer, W. and Karschin, A. (1996) J. Neurosci. 16, 3559–3570.
[15] Paxinos, G. and Watson, C. (1996) Academic Press, San Diego, CA.
[16] Mouri, T., Kittaka, N., Horio, Y., Copeland, N.G., Gilbert, D.J., Jenkins, N.A. and Kurachi, Y. (1998) Genomics 54, 181–182.
[17] Kubo, Y., Baldwin, T.J., Jan, Y.N. and Jan, L.Y. (1993) Nature 362, 127–133.
[18] Bredt, D.S., Wang, T.L., Cohen, N.A., Guggino, W.B. and Snyder, S.H. (1995) Proc. Natl. Acad. Sci. USA 92, 6753–6757.
[19] Périer, F., Radeke, C.M. and Vandenberg, C.A. (1994) Proc. Natl. Acad. Sci. USA 91, 6240–6244.
[20] Töpert, C., Döring, F., Wischmeyer, E., Karschin, C., Brockhaus, J., Ballanyi, K., Derst, C. and Karschin, A. (1998) J. Neurosci. 18, 4096–4105.
[21] Redell, J.B. and Tempel, B.L. (1998) J. Biol. Chem. 273, 22807–22818.
[22] Kowalski, J.M., Parekh, R.M., Mao, J. and Wittrup, K.D. (1998) J. Biol. Chem. 273, 19453–19458.
[23] Zerangue, N., Schwappach, B., Jan, Y.N. and Jan, L.Y. (1999) Neuron 22, 537–548.
[24] Sharma, N., Crane, A., Clement IV, J.P., Gonzalez, G., Babenko, A.P., Bryan, J. and Aguilar-Bryan, L. (1999) J. Biol. Chem. 274, 20628–20632.
[25] Morishige, K.I., Takahashi, N., Findlay, I., Koyama, H., Zanelli, J.S., Peterson, C., Jenkins, N.A., Copeland, N.G., Mori, N. and Kurachi, Y. (1993) FEBS Lett. 336, 375–380.
[26] Derst, C., Döring, F., Preisig-Müller, R., Daut, J., Karschin, A., Jeck, N., Weber, S., Engel, H. and Grzeschik, K.H. (1998) Genomics 54, 560–563.
[27] Hugnot, J.P., Pedeutour, F., Le Calvez, C., Grosgeorge, J., Passage, E., Fontes, M. and Lazdunski, M. (1997) Genomics 39, 113–116.
[28] Namba, N., Mori, R., Tanaka, H., Kondo, I., Narahara, K. and Seino, Y. (1997) Cytogenet. Cell. Genet. 79, 85–87.
[29] Tanemoto, M., Kittaka, N., Inanobe, A. and Kurachi, Y. (2000) J. Physiol. 525, 587–592.
[30] Tucker, S.J., Imbrici, P., Salvatorre, L., D'Adamo, M.C. and Pessia, M. (2000) J. Biol. Chem. 275, 16404–16407.
[31] Takumi, T., Ishii, T., Horio, Y., Morishige, K.I., Takahashi, N. and Yamada, M. et al. (1995) J. Biol. Chem. 270, 16339–16346.